Exosomal Transfer of MiR-500a-3p Confers Cisplatin Resistance and Stemness via Targeting FBXW7 in Gastric Cancer

Hao Lin
Department of General Surgery, Affiliated Xuzhou Hospital of Dongnan University Medical College, Xuzhou

Caihua Zhang
Department of General Surgery, Affiliated Xuzhou Hospital of Dongnan University Medical College, Xuzhou

Liang Zhang
Department of General Surgery, Affiliated Xuzhou Hospital of Dongnan University Medical College, Xuzhou

pengpeng liu (liupengpengxz@163.com)
xuzhou hospital https://orcid.org/0000-0003-3270-5630

Research

Keywords: exosome, chemoresistance, cisplatin, miRNA-500a-3p, gastric cancer

Posted Date: March 13th, 2020

DOI: https://doi.org/10.21203/rs.3.rs-17160/v1

Abstract

Background Chemoresistance has become a major obstacle for gastric cancer (GC) therapy in clinical practice. MiRNAs have been reported to play critical roles in the development of chemoresistance in various tumors, including GC. However, the role of MiR-500a-3p within exosomes in cisplatin-resistant GC cells remains largely unknown.

Materials and methods Cell proliferation and exosome delivery assays were performed using CCK-8 and transwell assays, respectively. CD63, CD81, β-tubulin, FBXW7, GAPDH, CD133, CD44 and SOX2 were detected by western blot and immunofluorescence assays. The expression levels of miR-500a-3p and FBXW7 mRNA were measured by real-time qRT-PCR. The interaction between miR-500a-3p and FBXW7 was predicted by bioinformatics software and confirmed by the dual-luciferase reporter. The mechanism of exosomal miR-500a-3p for cisplatin resistance was investigated in vitro and in vivo experiments.

Results MiR-500a-3p level was upregulated in cisplatin-resistant GC cells and its downregulation enhanced cisplatin sensitivity. Moreover, extracellular miR-500a-3p could be incorporated into exosomes and transmitted to sensitive cells, thus disseminating cisplatin resistance. Additionally, exosomal miR-500a-3p promoted cisplatin resistance via targeting FBXW7 in vitro and in vivo . Clinically, higher expression of miR-500a-3p in the plasma exosomes of GC patients is correlated with DDP resistance and thereby results in poor progression-free prognosis.

Conclusion Our finding highlights the potential of exosomal miR-500a-3p as an alternative modality for the prediction and treatment of GC with chemoresistance, providing a novel avenue for the treatment of GC.

Background

Gastric cancer (GC) is a serious global public health problem that rank the sixth most common malignancy and the third leading cause of cancer-related deaths worldwide[1]. Due to most GC patients diagnosed in advanced or metastatic stages[2], chemotherapy becomes the main strategy to improve prognosis and mitigate adverse symptoms, such as gastric bleeding or obstruction[3]. In this regard, cisplatin(DDP) is still one of the most used drugs in first-line chemotherapy against advanced GC[4]. However, chemoresistance—whether intrinsic or acquired—remains an inevitable obstacle in most GC patients and represents the most important cause of recurrence and mortality in GC[5].

Exosomes have been identified as an important group of 30–100 nm sized extracellular vesicles with lipid bilayer membranes and cup-shaped constructio[6]. When endosomal multivesicular bodies fuse with the cell membrane, exosomes carrying biomolecules including lipids, proteins and RNAs can be released into the extracellular environment[7–9]. After uptake of exosomes by neighboring or distant recipient cells, the exosomal contents exhibit biological activities such as immunomodulation[10], angiogenesis[11], autophagy[12], stem cell differentiation[13] and intercellular communication[14]. While in cancer research, a plethora of recent evidence indicates that exosomes participate in tumor

microenvironment remodeling, angiogenesis, invasion, metastasis and chemoresistance through initiating or suppressing various signaling pathways in the recipient cells[15]. RNA cargo that protected by exosomes from digestion has garnered much attention from researchers, especially microRNAs(miRNAs). MiRNAs are a class of 18–22 nucleotides small single-stranded non-coding RNA molecules that promote mRNA cleavage and subsequent degradation by binding to the complementary 3' untranslated region (UTR) of the mRNA and thereby regulate protein regulation[16]. Emerging evidence has demonstrated that tumor cell-secreted exosomal miRNAs play a crucial role in regulating tumor growth, metastasis, angiogenesis and chemoresistance[17–20]. However, the mechanisms of exosomeal miRNAs in DDP resistant GC are still waiting for exposure.

In this study, the effect of exosome-transmitted miRNAs on DDP resistance in GC cells was investigated. Moreover, we identify exosomal miR-500a-3p promote DDP resistance and CSCs properties in GC cells by downregulating FBXW7. Clinically, miR-500a-3p expression correlated positively with DDP resistance as well as recurrence and might be a potential therapeutic predictor of DDP-based chemotherapy in GC patients.

Methods

Cell culture

GC cell lines MGC803 and MKN45 were obtained from the ATCC. They have been authenticated by a STR(Short TandemRepeat) DNA profiling analysis and routinely examined for Mycoplasma contamination. Both cell lines were maintained in RPMI 1640(HyClone, Logan, UT, USA) with 10% fetal bovine serum (FBS; Thermo Fisher Scientific, Waltham, MA, USA), penicillin (100 U/mL) and streptomycin (100 mg/mL) (Invitrogen, Carlsbad, CA, USA). Continuous exposure to stepwise-enhancing concentrations of DDP (Sigma-Aldrich, St. Louis, MO, USA) was used to establish DDP resistant MGC803(MGC803/DDP) and MKN45(MKN45/DDP) cells. Briefly, these cells were initially cultured in medium with a relatively low concentration of DDP (0.1 μM) for 6 weeks. Subsequently, the surviving cells were exposed to higher concentration of DDP (0.2, 0.4, 0.8, 1.6 μM) for 6 weeks gradually. Lastly, MGC-803 and MKN-45 cells were incubated in the culture medium containing a high concentration of DDP (3.0 μM). All cells were grown in a moist atmosphere with 5% carbon dioxide incubator at 37 °C.

Patient samples and ethical statement

Plasma samples were collected from 55 III stage GC patients receiving DDP-based chemotherapy after gastrectomy with D2 lymphadenectomy at Affiliated Xuzhou Hospital of Dongnan University Medical College. The patients were allocated into the chemoresistant group (n = 25) and chemosensitive group (n = 30) according to the Response Evaluation Criteria in Solid Tumors criteria. This research was carried out with approval of Research Ethics Committee of Xuzhou Hospital. All participants gave written informed consent before blood sample collection

Exosome isolation and purification

An ExoQuick precipitation kit (System Biosciences, LLC, Palo Alto, CA) was used to extract and purify exosomes in accordance with the manufacturer's instruction. Briefly, the culture medium or plasma was harvested and centrifuged at 3,000 g for 15 min for removing cell debris. The obtained supernatant was then mixed with ExoQuick precipitation solution, followed by incubation at 4 °C for 30 min and centrifugation at 1,500 g for 30 min. After carefully removing the supernatant with a pipette, the exosome pellets participated in the bottom were centrifuged for another 5 min at 1,500 g to remove the extra liquid. Finally, the exosome pellets were resuspended in 100 μl phosphate-buffered saline (PBS).

Characterization of exosomes

The morphology of exosome was observed by transmission electron microscopy. Briefly, Exosomes in PBS were fixed using 1% glutaraldehyde and incubated at 4 °C. Then, 10 μl of the suspension was placed onto formvar/carboncoated copper grids, followed by dyeing with 3% aqueous phospphotungstic aid for 30 seconds. Subsequently, exosomes were observed with a transmission electron microscopy (TEM; Tecnai 12; Philips). Size distribution of exosomes was analyzed by NanoSight LM10 system which was equipped with a fast video capture and particle-tracking software (NanoSight, Amesbury, UK). Western blot analysis was performed to detect exosome markers CD63 and CD81.

Exosomes and miR-500a-3p internalization assays

Exosomes were labeled with PKH-67 green fluorescent Cell Linker Kit for General Cell Membrane Labeling (Sigma-Aldrich) according to the manufacturer's protocol. Then, the labeled exosomes were incubated with MGC803 cells for 30 hours at 37 °C. For the transfer of exosomal miR-500a-3p, PKH-67 labeled miR-500a-3p was transfected to MGC803 cells by liposome 2000 (Invitrogen, CA, USA). The PKH-67-miR-301a-expressing MGC803 cells were grown on the 0.4 mm pore size transwell (Thermo Fisher Scientific) and then co-cultured with MGC803 cells that had been grown on the cover slips in the bottom well of the transwell for 30 hours. The uptake of labeled exosomes or miR-500a-3p by the recipient MGC803 cells was observed using a Nikon Eclipse fluorescence microscope (Nikon, Tokyo, Japan).

Cell Proliferation Assay

Cell Counting Kit-8 (CCK-8; Sangon Biotech, Shanghai, China) was applied to examine cell proliferation ability. Briley, transfected or exosomes-treated GC cells were inoculated into 96-well plates and exposed to varying doses of DDP for 30 hours. Subsequently, cell viability was examined by CCK-8 following the manufacture's specification. Finally, the absorbance of test wells was read under a microplate reader (Bio-Rad, Hercules, CA, USA) at 450 nm. Half-maximal inhibitory concentration (IC_{50}) values were calculated on the basis of the charted dose-response curve from GraphPad Prism 5.0 software.

Immunofluorescence assay

Transfected or exosomes-treated GC cells were fixed in 4% paraformaldehyde for 10 min, blocked with PBS buffer containing 5% bovine serum albumin. Then those cells incubated with antibodies at 4 °C

overnight, followed by incubation with fluorescein isothiocyanate (FITC)-conjugated secondary antibody and the nuclear counterstain diaminophenylindole (DAPI). After rinsing, the cells were analyzed using immunofluorescence microscopy.

Sphere formation assay

Transfected or exosomes-treated GC cells were plated in each well of ultra-low-attachment 24-well plates (Corning Life Sciences, Corning, NY, USA) at low density (500 cells per each well) with 0.8% methyl cellulose (Sigma, USA) supplemented with 20 μl/ml B27 supplement (Life Technologies), 20 ng/ml basic fibroblast growth factor (bFGF, Gibco), 10 ng/ml EGF (Gibco), LIF (Gibco), 1% L-glutamine (Gibco) and 1% penicillin-streptomycin sulfate (Thermo Fisher Scientific) for 2 weeks. The number of sphere in each well ≥ 50 μm in diameter were counted under a microscope. Sphere formation rate for each well was the ratio of colony number to total cell number per well.

Western blot assay

Proteins were extracted with a lysis buffer and then quantified by a bicinchoninic acid protein assay. Equivalent amounts of cell lysates were separated using SDS-PAGE and transferred to a polyvinylidene difluoride membrane (Roche Applied Sciences). Membranes were immunoblotted overnight at 4 °C with antibodies, followed by the appropriate second antibodies(supplement table 1). The bands were visualized using Pierce ECL Western Blotting Substrate (Thermo Fisher Scientific). Image density of the immunoblotting was determined by Gel densitometry (Bio-Rad).

RNA extraction, and real-time qRT-PCR

Total RNA for cultured cells and exosomes were extracted with using Trizol Reagent (Takara Bio, Inc., Shiga, Japan). The mRNA expressions were detected by the PrimeScript RT Reagent Kit and SYBR Premix Ex Taq (Takara Bio, Inc., Shiga, Japan). GAPDH was used as control. All the primers designed for qPCR were listed in supplemental table 1. All-in-One microRNA qRT-PCR Detection Kits (GeneCopoeia, Inc., Maryland, USA) were used to detect miRNA expression and U6 used as a control. Every experiment was repeated 3 times according to the manufacturer's protocol. Final data were analyzed with the 2-ΔΔCt method.

Luciferase assays

For luciferase reporter assays, the 293T cells were cotransfected with wild-type or mutant FBXW7 3'UTR psiCHECK-2 plasmid (Promega) and mimic-miR-500a-3p or anti-miR-500a-3p(Ribo) or control using Lipofectamine 2000 (Invitrogen). Luciferase activity was measured 48 hours after transfection by the Dual-luciferase Reporter Assay System (Promega). Firefly luciferase signal was used for normalization. Each assay was repeated in three independent experiments.

Plasmid construction and RNA transfection

Mimic, anti-miRNA-500a-3p, scrambled control were obtained from GenePharma and were transfected at a final concentration of 100 nM. For FBXW7 overexpression, PCRamplified full-length human FBXW7 cDNA was cloned into pcDNA3.1 (pcDNA3.1- FBXW7) and transfected to GC cells via Lipofectamine 2000 (Invitrogen; Thermo Fisher Scientific, Inc.) as the delivery agent, according to the manufacturer's protocol.

Abdominal tumorigenicity assay in vivo

All animal experiments were conducted in accordance with the principles and procedures approved by the Committee on the Ethics of Xuzhou hospital. In BALB/c nude mice model, 5×10^6 GC cells, including DDP resistant or not or FBXW7-expression plasmid transfected, were injected into the abdominal cavity for tumorigenicity (n = 5 in each group) and then indicated treatment such as PBS, exosomes or conditioned medium(CM) without exosomes would be injected into abdominal cavity every 5 days. Meanwhile, all mice were administrated DDP(2 mg/kg) by abdominal injection after above treatment. Tumor growth was monitored and quantified using an IVIS-100 system (Caliper Life Sciences,Boston, MA, USA) every 5 days. Twenty days later, all mice were sacrificed after luciferase signal intensity examination and the xenograft tumor were subjected to H&E staining.

Statistics

All in vitro experiments were repeated at least in triplicate. The data was represented as either a scatter plots or bar graphs with means ± standard error deviation of the mean (SEM). The statistical analysis was performed using SPSS software (version 13.0, NY, USA). Statistical significance between two groups was determined using a two-tailed Student's t-test. To compare multiple groups, one-way analysis of variance (ANOVA) followed by a Bonferroni-Dunn test was performed. The GC patients were divided into high expression group and low expression group according to the median ofmiR-500a-3p expression and Kaplan-Meier survival analysis was implemented to compare GC patient progression-free surviva by log-rank test. The receiver operating characteristic (ROC) curve was applied to determine the area under the curve (AUC) values for exosomal miR-500a-3p in plasma by the GraphPad Prism Software (GraphPad Software, Inc., San Diego, CA). $P < 0.05$ was considered statistically significant.

Result

DDP resistant GC cells exhibited higher tumorigenesis and CSCs properties

To explore the underlying regulatory mechanism of GC DDP resistance, DDP-resistant cell lines, MGC803/DDP and MKN45/DDP, were established by treating MGC803 and MKN45 cells with gradually elevating doses of DDP in successive passages. First of all, we examined the cell viability and IC_{50} values in MGC803, MGC803/DDP and MKN45, MKN45/DDP by exposing them to different concentrations of DDP for 30 hours. As shown in Fig. 1A and B, compared to MGC803 and MKN45 cells, MGC803/DDP and MKN45/DDP presented higher cell viability and IC_{50} value. Furthermore, both MGC803/DDP(Fig. 1C and E) and MKN45/DDP(Fig. 1D and F) exhibited enhanced abdominal tumorigenesis and more metastatic nodules compared to their corresponding parental cells. Accumulating evidences demonstrate that CSCs

play important roles in chemoresistance of many human tumors. In our established DDP resistant GC cells lines, higher proportion of CSCs markers CD133+, CD44 + and SOX + were observed in MGC803/DDP and MKN45/DDP cells(Fig. 1G). Consistently, MGC803/DDP and MKN45/DDP cells could formed larger spheres compared to those sensitive cells(Fig. 1H). These data suggested that DDP resistant GC cells have been successfully constructed and those DDP resistant GC cells exhibited higher tumorigenesis and CSCs properties.

MGC803/DDP-derived exosomes conferred DDP resistance and promote CSCs properties in recipient MGC803 cells

Recent studies revealed that exosomes secreted by cancer cells were implicated in chemotherapy resistance[19, 20]. We speculated that exosomes from DDP resistant GC cells might exert their effects on recipient cells. In order to verify this conjecture, we isolated exosomes from the conditioned medium(CM) of MGC803 and MGC803/DDP cells. Transmission electron microscopy(TEM) revealed a cup-shaped vesicles with bilayered membranes and the Nanosight particle tracking analysis (NTA) further identified that the predominant size of the vesicles was 100 nm(Fig. 2A), that are typical exosomes. Moreover, MGC803/DDP cells secreted significantly more exosomes than MGC803 cells(Fig. 1B). By western blot analysis, the exosomal markers CD63, CD81 were detected in the exosomes, whereas β-tubulin was enriched in the whole cell lysates (Fig. 2C). After that, PHK-67 labled MGC803 and MGC803/DDP exosomes(green fluorescence) were cocultured with MGC803 CM. As expected, green fluorescence signals were observed in exosomes treated MGC803 cells while no signal in PBS treated cells(Fig. 2D). The uptake efficiency of exosomes by MGC803 cells escalated in a time-dependent manner and more than 80% cells were positive for PKH67 fluorescence at 24 h(Fig. 2E). Thereby, we examined the effects of MGC803/DDP exosomes in DDP resistance in vivo and in vitro. Proliferation assay showed that MGC803/DDP exosomes increased MGC803 cell viability and IC_{50} values compared to PBS or MGC803 exosomes(Fig. 2F). In MGC803 cells abdominal tumorigenesis assay, MGC803/DDP exosomes accelerate tumor growth and dissemination under DDP therapy(Fig. 2G-I). Besides, the sphere formation capability(Fig. 2J) and CSCs properties(Fig. 2K) of MGC803 cells increased when coculturing with exosomes from MGC803/DDP rather than MGC803. These results indicated that the vesicles isolated from MGC803 and MGC803/DDP display typical characteristics of exosomes and that exosomes from MGC803/DDP contributed to disseminate DDP resistance and promote CSCs properties in recipient MGC803 cells.

MGC803/DDP-derived exosomes enhances DDP resistance of MGC803 recipient cells via exosome-mediated delivery of miR-500a-3p in vitro and in vivo

Next, we compared the expression of miR-500a-3p in MCG803, MGC803/DDP and their secreted exosomes. As shown in Fig. 3A and B, miR-500a-3p expression were significantly higher both in MGC803/DDP and their secreted exosomes by real time qRT-PCR. Thus, we assumed that miR-500a-3p from MGC803/DDP exosomes may confer DDP resistance to recipient MGC803 cells via exosome transfer. In the coincubation experiments, MGC803 intracellular miR-500a-3p levels were dramatically

upregulated upon incubation with exosomes from MGC803/DDP with miR-500a-3p higher expression but not with exosomes from MGC803/DDP with miR-500a-3p knockdown by anti-miR-500a-3p transfection(Fig. 3C). While incubation with exosomes from MGC803 with miR-500a-3p overexpression by mimic-miR-500a-3p increased MGC803 intracellular miR-500a-3p level(Fig. 4D). Functionally, MGC803 cells became insensitive to DDP when incubated with exosomes with higher miR-500a-3p, whereas miR-500a-3p downregulation in exosomes abolished this effect(Fig. 3C, D). Moreover, the elevation of miR-500a-3p in recipient cells exhibited a time-dependent manner after incubation with MGC803/DDP exosomes(Fig. 3E). However, the level of pre- miR-500a-3p (precursor of miR-500a-3p) was not changed when incubating with MGC803/DDP exosomes(Fig. 3F), suggesting the miR-500a-3p elevation in recipient cells was not the result of miRNA endogenous synthesis but more likely a direct transfer by exosomes. Subsequently, we found miR-500a-3p expression in MGC803/DDP CM was little changed upon RNase A treatment but significantly decreased when treated with RNase A + Triton X-100 simultaneously (Fig. 3G), indicating that extracellular miR-500a-3p was mainly encased within the membrane instead of directly released. To visualize miR-500a-3p transfer, MGC803 and MGC803/DDP cells transiently transfected with PHK67-tagged miR-500a-3p were cocultured with MGC803 cells for 30 hours in a transwell system, as depicted in Fig. 3H. As a result, the green fluorescently labeled miR-500a-3p was observed in the lower chamber cells through confocal microscopy (Fig. 3H), further suggesting that miR-500a-3p could be transferred by exosomes. In abdominal tumorigenesis model, MGC803/DDP exosomes promoted tumor growth and dissemination under DDP therapy but downregulating miR-500a-3p in MGC803/DDP exosomes could abolished its tumor promoting effect(Fig. 3I-K). These findings revealed that functional exosomal miR-500a-3p from DDP resistant GC cells could be transferred to recipient ones, which subsequently became resistant to DDP in vivo and in vitro.

MGC803/DDP-derived exosomal miR-500a-3p confers DDP resistance in recipient MGC803 cells via inhibiting FBXW7

By the publicly available algorithms TargetScan and mirDIP 4.1, we found that FBXW7 was the potential downstream targets of miR-500a-3p with high predictive values. To substantiate the site-specific repression of miR-500a-3p on FBXW7, we constructed wide type and mutated FBXW7 3'-UTR luciferase reporter according to TargetScan algorithm. Dual-luciferase activity assay showed that the luciferase activity of FBXW7 with wild type 3’UTR was significantly inhibited in mimic-miR-500a-3p transfected 293T, whereas anti-miR-500a-3p specifically abolished this suppression. Moreover, mutations in the miR-500a-3p binding seed region of the FBXW7(LUC-FBXW7-Mutant) abrogated these above effects of mimic- or anti-miR-500a-3p transfection(Fig. 4A). Moreover, both mRNA and protein expression of FBXW7 were significantly decreased in MGC803 cells transfected with mimic-miR-500a-3p or cocultured with MGC803/DDP exosomes while reintroduction of FBXW7 abolished the miR-500a-3p upregulation or MGC803/DDP exosomes induced FBXW7 decrease(Fig. 4B-D). To further elucidate the functional role of FBXW7 in miR-500a-3p mediated DDP resistance, we constructed FBXW7-expressing plasmid. In proliferation assay, reintroduction of FBXW7 in MGC803 cells could reverse miR-500a-3p mediated DDP resistance. MGC803 abdominal tumorigenesis assay further revealed that reintroduction of FBXW7

suppressed tumor growth and dissemination under DDP therapy. Collectively, these results suggested that exosomal miR-500a-3p promoted DDP resistance in MGC803 cells through FBXW7 downregulation.

FBXW7 reversed the DDP resistance of exosomal miR-500a-3p by inhibiting CSCs properties

To determine the potential mechanisms underlying the role of FBXW7 in abrogating the DDP resistance by miR-500a-3p, we investigated the CSCs properties in GC. In sphere formation assay, MGC803/DDP exosomes induced more number and size of sphere formation were abrogated by FBXW7 overexpression(Fig. 5A and B). Additionally, upregulation of cell stemness markers CD133, CD44 and SOX2 by MGC803/DDP exosomes could be inhibited by reintroduction of FBXW7(Fig. 5C-F). These above data demonstrated that exosomal miR-500a-3p/ FBXW7 axis enhances DDP resistance in MGC803 cells by CSCs properties activation.

Plasma exosomal miR-500a-3p is related to DDP resistance in III stage GC patients

Clinically, we investigated the plasma exosomal miR-500a-3p level in III stage GC patients who would receive DDP-based chemotherapy. As presented in Fig. 6A, plasma exosomal miR-500a-3p levels were significantly higher in DDP resistant patients than in that of sensitive patients. Moreover, Kaplan-Meier analysis revealed that high exosomal miR-500a-3p levels in III stage GC patient plasma were correlated with reduced overall survival(Fig. 6B). Importantly, receiver operating characteristic (ROC) curve analysis demonstrated that the ability to discriminate between the resistant and sensitive group with the plasma exosomal miR-500a-3p level was acceptably accurate(AUC = 0.843, Fig. 6C). Above all, the plasma exosomal miR-500a-3p might be applied as the noninvasive biomarker for DDP resistance in GC.

Discussion

In spite of DDP-based chemotherapy is particularly effective in a large number of cancers, the emerge of DDP resistance has become a main obstacle for the treatment of cancer patients[21, 22], especially in GC[23, 24]. The platinum compound DDP can bind covalently to DNA, forming adducts that inhibit DNA replication subsequently causing transcription inhibition, cell-cycle arrest, DNA repair deficiency and apoptosis[25]. Unfortunately, the overall 5-year survival rate for GC patients who received DDP based chemotherapy after surgery remains dismal, while for late stage cases, DDP has shown little benefits due to dissatisfactory treatment efficiency, resulting in tumor progression and reduced prognosis[5]. Therefore, investigating the molecular mechanisms underlying DDP resistance may be of great significance for improving GC patient outcome[4, 26, 27]. In current study, the effects and mechanism of exosomal miR-500a-3p in DDP resistance were explored in GC cell. Our data suggested that miR-500a-3p abundance was elevated in DDP resistant GC cells and their secreted exosomes. Moreover, we found that exosomal miR-500a-3p could contribute to DDP resistance in recipient GC cells by downregulating FBXW7 expression via enhancing stemness cells properties.

There have been several reports showing that chemotherapy are capable to stimulate cancer cells to release more exosomes[28, 29]. Lv et al. reported that certain drugs such as paclitaxel, irinotecan and

carboplatin could significantly elevate the abundance of exosomes released from HepG2 (hepatocellular carcinoma cells)[30]. In breast cancer, Kreger et al. found that, compared to those untreated MDA-MB231 cells, the number of exosomes shed by the MDA-MB231 cells increased after paclitaxel treatment[31]. Besides in vitro model, paclitaxel was reported to induce a higher release of exosomes in 4T1-bearing mice and even in breast cancer patients, it was discovered that more exosomes were secreted after post-neoadjuvant chemotherapy as compared to the basal levels by NTA[32, 33]. Similar to above mentioned references, our study showed that DDP resistant cells(MGC803/DDP and MKN45/DDP) could release more exosomes than their parental ones. The higher exosomes release induced by chemotherapy is probably due to the cellular stress and damage resulted from chemotherapy. This process are resembling to how cells release damage associated molecular patterns (DAMPs)[34, 35].

Recently, miRNAs have been reported to be encapsulated in tumor-derived exosomes to avoid degradation and subsequently those exosomal miRNAs would transfer to recipient cells and change their phenotypes via regulating genes expression, including angiogenesis, invasion and metastasis[36, 37]. While for chemoresistance, drug-resistant cells may release exosomal miRNAs into the microenvironment and confer drug resistance to recipient cells[38, 39]. Exosomal miR-196a derived from cancer associated fibroblasts confers DDP resistance in head and neck cancer through targeting CDKN1B and ING5[38]. Exosomal miR-126a have been reported to be involved in the doxorubicin resistance of lung cancer[19]. MiR-32-5p is delivered from HCC multidrug-resistant cells to sensitive cells via exosomes and activates the PI3K/Akt pathway to induce multidrug resistance[20]. Our results proved that exosomes from DDP resistant GC cells enhances recipient cells resistance to DDP by miR-500a-3p/FBXW7 pathway in vitro and in vivo.

MiR-500a-3p has been reported to be implicated in the chemotherapeutic resistance, invasion and migration via GSK-3β and LY6K in different types of cancers[40–42]. However, the biological roles of miR-500a-3p and the underlying molecular mechanisms responsible for GC have not been reported. In this study, we found that miR-500a-3p was elevated in exosomes from DDP resistant GC cells and clinical upregulation of miR-500a-3p in exosomes from III stage GC patients' plasma correlated with DDP-based chemoresistance and GC progression, which might be used as a noninvasive predictor of chemotherapy in GC Patients. Furthermore, FBXW7 was identified as the target of miR-500a-3p in GC. FBXW7(F-box with 7 tandem WD40) is one of the crucial components of ubiquitin ligase that aids in the degradation of many oncoproteins via the ubiquitin-proteasome system. FBXW7 is considered as a potent tumor suppressor in different human cancers, as most of its target substrates can function as potential growth promoters[43]. For instance, FBXW7 inactivation sensitized cancer cells to radiation or etoposide by stabilizing p53 to induce cell-cycle arrest and apoptosis[44]. While in GC, low expression of FBXW7 was observed in primary GC and contributed to the poor survival and minimal response to adjuvant therapy[45]. Downregulation of FBXW7 by miR-223 in GC cells promote proliferation, invasion and chemoresistance to trastuzumab in vitro[46, 47]. Here we found that overexpression of FBXW7 suppressed exosomal miR-500a-3p induced CSCs properties and thus reversed exosome mediated DDP resistance in GC.

Conclusion

In sammary, we provide evidence that DDP resistance GG cells can secret miR-500a-3p enriched exosomes to promote stemness and DDP resistance by targeting FBXW7 in GC cells (Fig. 6D). Moreover, exosomal miR-500a-3p is up-regulated in the plasma of GC patients with DDP resistance, which thereby results in poor progression-free prognosis. We envision that blocking the function of exosomal miR-500a-3p could be potentially used as an alternative modality for the prediction and treatment of GC with chemoresistance.

Declarations

Availability of Data and Materials

The data used to support findings of the study are available from the corresponding author upon request.

Ethics Approval and Consent to Participate

The study was approved by the medical ethics committee of Affiliated Xuzhou Hospital of Dongnan University Medical College.

Consent for Publication

We have received consent from individual patients who have participated in this study. The consent forms will be provided upon request.

Author contributors

H.L. and C.Z. performed primer design and experiments. L.Z. and P.L. contributed to the animal experiments. H.L. contributed to RT-PCR and qRT-PCR. P.S. analyzed the data. L.Z. and P.L. wrote the paper. All authors read and approved the final manuscript.

Conflicts of interest

The authors declare they have no competing interests.

Funding

Not applicable

Acknowledgements

Not applicable

References

1. Bray F, Ferlay J, Soerjomataram I *et al*: **Global cancer statistics 2018: GLOBOCAN estimates of incidence and mortality worldwide for 36 cancers in 185 countries**. *CA Cancer J Clin* 2018, **68**(6):394-424.
2. Marin JJ, Al-Abdulla R, Lozano E *et al*: **Mechanisms of Resistance to Chemotherapy in Gastric Cancer**. *Anticancer Agents Med Chem* 2016, **16**(3):318-334.
3. Zhang D, Fan D: **New insights into the mechanisms of gastric cancer multidrug resistance and future perspectives**. *Future Oncol* 2010, **6**(4):527-537.
4. Keehn RJ, Higgins GA, Jr.: **Chemotherapy for gastric cancer**. *Lancet* 1981, **1**(8215):323.
5. Shi WJ, Gao JB: **Molecular mechanisms of chemoresistance in gastric cancer**. *World J Gastrointest Oncol* 2016, **8**(9):673-681.
6. Kahroba H, Hejazi MS, Samadi N: **Exosomes: from carcinogenesis and metastasis to diagnosis and treatment of gastric cancer**. *Cell Mol Life Sci* 2019, **76**(9):1747-1758.
7. Kowal J, Tkach M, Thery C: **Biogenesis and secretion of exosomes**. *Curr Opin Cell Biol* 2014, **29**:116-125.
8. Sousa D, Lima RT, Vasconcelos MH: **Intercellular Transfer of Cancer Drug Resistance Traits by Extracellular Vesicles**. *Trends Mol Med* 2015, **21**(10):595-608.
9. Thery C, Zitvogel L, Amigorena S: **Exosomes: composition, biogenesis and function**. *Nat Rev Immunol* 2002, **2**(8):569-579.
10. Robbins PD, Morelli AE: **Regulation of immune responses by extracellular vesicles**. *Nat Rev Immunol* 2014, **14**(3):195-208.
11. Teng X, Chen L, Chen W *et al*: **Mesenchymal Stem Cell-Derived Exosomes Improve the Microenvironment of Infarcted Myocardium Contributing to Angiogenesis and Anti-Inflammation**. *Cell Physiol Biochem* 2015, **37**(6):2415-2424.
12. Baixauli F, Lopez-Otin C, Mittelbrunn M: **Exosomes and autophagy: coordinated mechanisms for the maintenance of cellular fitness**. *Front Immunol* 2014, **5**:403.
13. Nair R, Santos L, Awasthi S *et al*: **Extracellular vesicles derived from preosteoblasts influence embryonic stem cell differentiation**. *Stem Cells Dev* 2014, **23**(14):1625-1635.

14. Tkach M, Thery C: **Communication by Extracellular Vesicles: Where We Are and Where We Need to Go**. *Cell* 2016, **164**(6):1226-1232.
15. Mashouri L, Yousefi H, Aref AR *et al*: **Exosomes: composition, biogenesis, and mechanisms in cancer metastasis and drug resistance**. *Mol Cancer* 2019, **18**(1):75.
16. Bartel DP: **MicroRNAs: target recognition and regulatory functions**. *Cell* 2009, **136**(2):215-233.
17. Valadi H, Ekstrom K, Bossios A *et al*: **Exosome-mediated transfer of mRNAs and microRNAs is a novel mechanism of genetic exchange between cells**. *Nat Cell Biol* 2007, **9**(6):654-659.
18. Wei F, Ma C, Zhou T *et al*: **Exosomes derived from gemcitabine-resistant cells transfer malignant phenotypic traits via delivery of miRNA-222-3p**. *Mol Cancer* 2017, **16**(1):132.
19. Deng Z, Rong Y, Teng Y *et al*: **Exosomes miR-126a released from MDSC induced by DOX treatment promotes lung metastasis**. *Oncogene* 2017, **36**(5):639-651.
20. Fu X, Liu M, Qu S *et al*: **Exosomal microRNA-32-5p induces multidrug resistance in hepatocellular carcinoma via the PI3K/Akt pathway**. *J Exp Clin Cancer Res* 2018, **37**(1):52.
21. Galluzzi L, Senovilla L, Vitale I *et al*: **Molecular mechanisms of cisplatin resistance**. *Oncogene* 2012, **31**(15):1869-1883.
22. Chen J, Solomides C, Parekh H *et al*: **Cisplatin resistance in human cervical, ovarian and lung cancer cells**. *Cancer Chemother Pharmacol* 2015, **75**(6):1217-1227.
23. Hou G, Bai Y, Jia A *et al*: **Inhibition of autophagy improves resistance and enhances sensitivity of gastric cancer cells to cisplatin**. *Can J Physiol Pharmacol* 2020.
24. Lei Y, Tang L, Hu J *et al*: **Inhibition of MGMT-mediated autophagy suppression decreases cisplatin chemosensitivity in gastric cancer**. *Biomed Pharmacother* 2020, **125**:109896.
25. Wang D, Lippard SJ: **Cellular processing of platinum anticancer drugs**. *Nat Rev Drug Discov* 2005, **4**(4):307-320.
26. Hu T, Li Z, Gao CY *et al*: **Mechanisms of drug resistance in colon cancer and its therapeutic strategies**. *World J Gastroenterol* 2016, **22**(30):6876-6889.
27. Das M, Law S: **Role of tumor microenvironment in cancer stem cell chemoresistance and recurrence**. *Int J Biochem Cell Biol* 2018, **103**:115-124.
28. Bandari SK, Purushothaman A, Ramani VC *et al*: **Chemotherapy induces secretion of exosomes loaded with heparanase that degrades extracellular matrix and impacts tumor and host cell behavior**. *Matrix Biol* 2018, **65**:104-118.
29. Pascucci L, Cocce V, Bonomi A *et al*: **Paclitaxel is incorporated by mesenchymal stromal cells and released in exosomes that inhibit in vitro tumor growth: a new approach for drug delivery**. *J Control Release* 2014, **192**:262-270.
30. Lv LH, Wan YL, Lin Y *et al*: **Anticancer drugs cause release of exosomes with heat shock proteins from human hepatocellular carcinoma cells that elicit effective natural killer cell antitumor responses in vitro**. *J Biol Chem* 2012, **287**(19):15874-15885.

31. Kreger BT, Johansen ER, Cerione RA *et al*: **The Enrichment of Survivin in Exosomes from Breast Cancer Cells Treated with Paclitaxel Promotes Cell Survival and Chemoresistance**. *Cancers (Basel)* 2016, **8**(12).
32. Keklikoglou I, Cianciaruso C, Guc E *et al*: **Chemotherapy elicits pro-metastatic extracellular vesicles in breast cancer models**. *Nat Cell Biol* 2019, **21**(2):190-202.
33. Konig L, Kasimir-Bauer S, Bittner AK *et al*: **Elevated levels of extracellular vesicles are associated with therapy failure and disease progression in breast cancer patients undergoing neoadjuvant chemotherapy**. *Oncoimmunology* 2017, **7**(1):e1376153.
34. Fleshner M, Crane CR: **Exosomes, DAMPs and miRNA: Features of Stress Physiology and Immune Homeostasis**. *Trends Immunol* 2017, **38**(10):768-776.
35. Ab Razak NS, Ab Mutalib NS, Mohtar MA *et al*: **Impact of Chemotherapy on Extracellular Vesicles: Understanding the Chemo-EVs**. *Front Oncol* 2019, **9**:1113.
36. Yang F, Ning Z, Ma L *et al*: **Exosomal miRNAs and miRNA dysregulation in cancer-associated fibroblasts**. *Mol Cancer* 2017, **16**(1):148.
37. Sun Z, Shi K, Yang S *et al*: **Effect of exosomal miRNA on cancer biology and clinical applications**. *Mol Cancer* 2018, **17**(1):147.
38. Qin X, Guo H, Wang X *et al*: **Exosomal miR-196a derived from cancer-associated fibroblasts confers cisplatin resistance in head and neck cancer through targeting CDKN1B and ING5**. *Genome Biol* 2019, **20**(1):12.
39. Liu X, Lu Y, Xu Y *et al*: **Exosomal transfer of miR-501 confers doxorubicin resistance and tumorigenesis via targeting of BLID in gastric cancer**. *Cancer Lett* 2019, **459**:122-134.
40. Guo Y, Chen L, Sun C *et al*: **MicroRNA-500a promotes migration and invasion in hepatocellular carcinoma by activating the Wnt/beta-catenin signaling pathway**. *Biomed Pharmacother* 2017, **91**:13-20.
41. Liao XH, Xie Z, Guan CN: **MiRNA-500a-3p inhibits cell proliferation and invasion by targeting lymphocyte antigen 6 complex locus K (LY6K) in human non-small cell lung cancer**. *Neoplasma* 2018, **65**(5):673-682.
42. Jiang C, Long J, Liu B *et al*: **miR-500a-3p promotes cancer stem cells properties via STAT3 pathway in human hepatocellular carcinoma**. *J Exp Clin Cancer Res* 2017, **36**(1):99.
43. Sailo BL, Banik K, Girisa S *et al*: **FBXW7 in Cancer: What Has Been Unraveled Thus Far?** *Cancers (Basel)* 2019, **11**(2).
44. Cui D, Xiong X, Shu J *et al*: **FBXW7 Confers Radiation Survival by Targeting p53 for Degradation**. *Cell Rep* 2020, **30**(2):497-509 e494.
45. Li MR, Zhu CC, Ling TL *et al*: **FBXW7 expression is associated with prognosis and chemotherapeutic outcome in Chinese patients with gastric adenocarcinoma**. *BMC Gastroenterol* 2017, **17**(1):60.
46. Li J, Guo Y, Liang X *et al*: **MicroRNA-223 functions as an oncogene in human gastric cancer by targeting FBXW7/hCdc4**. *J Cancer Res Clin Oncol* 2012, **138**(5):763-774.

47. Eto K, Iwatsuki M, Watanabe M *et al*: **The sensitivity of gastric cancer to trastuzumab is regulated by the miR-223/FBXW7 pathway**. *Int J Cancer* 2015, **136**(7):1537-1545.

Figures

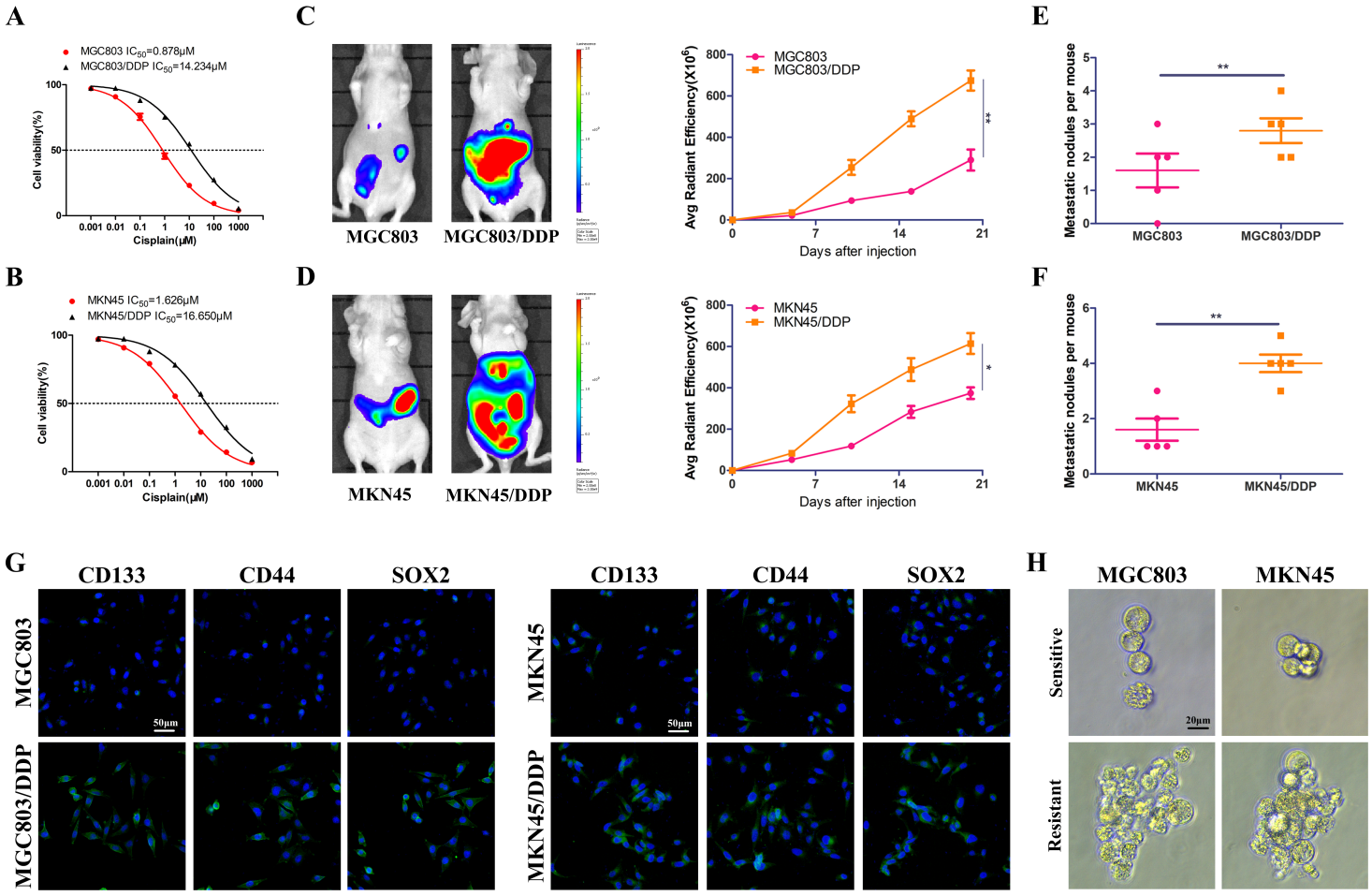

Figure 1

DDP (DDP) resistant MGC803 and MKN45 cells display stem cell-like features. A, B Proliferation assay analysis and IC50 value of DDP resistant GC cells (MGC803/DDP and MKN45/DDP) and corresponding parental cells (MGC803 and MKN45). C, D Representative images showed the bioluminescent signals of abdominal tumorigenesis by indicated GC cells under DDP treatment (left panel). Comparison of bioluminescent signals on the day 21 was analyzed(right panel), five nude mice in each group. E, F Comparison of abdominal metastatic nodules by indicated GC cells under DDP treatment. G Expression level of stemness markers CD133, CD44 and SOX2 in indicated GC cells by confocal microscopy. H Sphere formation assay in indicated GC cells. *p < 0.05, **p < 0.01.

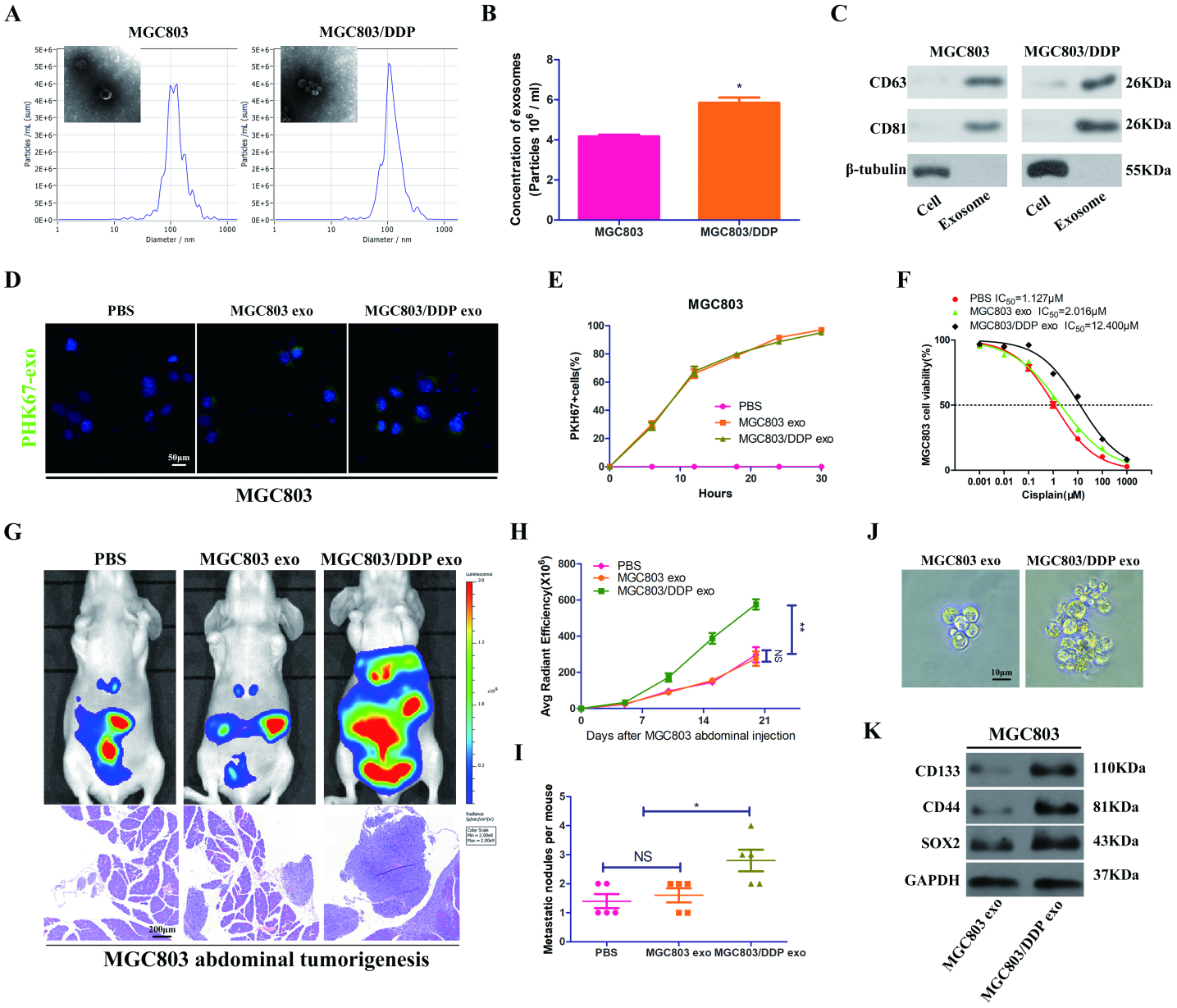

Figure 2

MGC803/DDP-derived exosomes disseminates DDP resistance and promote CSCs properties in recipient MGC803 cells. A Electron microscopy and NTA images of exosomes isolated from MGC803 and MGC803/DDP cells medium. B, C Identical quantity of MGC803 and MGC803/DDP cells were cultured 30 hours and then their exosomes concentrations and positive markers(CD63, HSP81) were analyzed by NTA(B) and western blot(C). D MGC803 cells were incubated with PHK-67-labled exosomes from MGC803 and MGC803/DDP cells for 30 hours, and the internalization of exosomes was detected by confocal microscopy. E Uptake efficiency of PHK-67-labled exosomes was examined by confocal microscopy. F Proliferation assay analysis and IC50 value of MGC803 cells cocultured with PBS, MGC830 exosomes or MGC803/DDP exosomes under DDP treatment. G Representative bioluminescent images and microscopy observations showed effects of PBS, MGC803 exosomes or MGC803/DDP exosomes on abdominal tumorigenesis under DDP treatment. H, I Comparison of bioluminescent signals and abdominal metastatic nodules after indicated treatment, five nude mice in each group. J, K Effect of

MGC803 exosomes and MGC803/DDP exosomes on sphere formation (J) and expression levels of stemness markers (K) in MCG803 cells by westen blot. *p < 0.05, **p < 0.01.

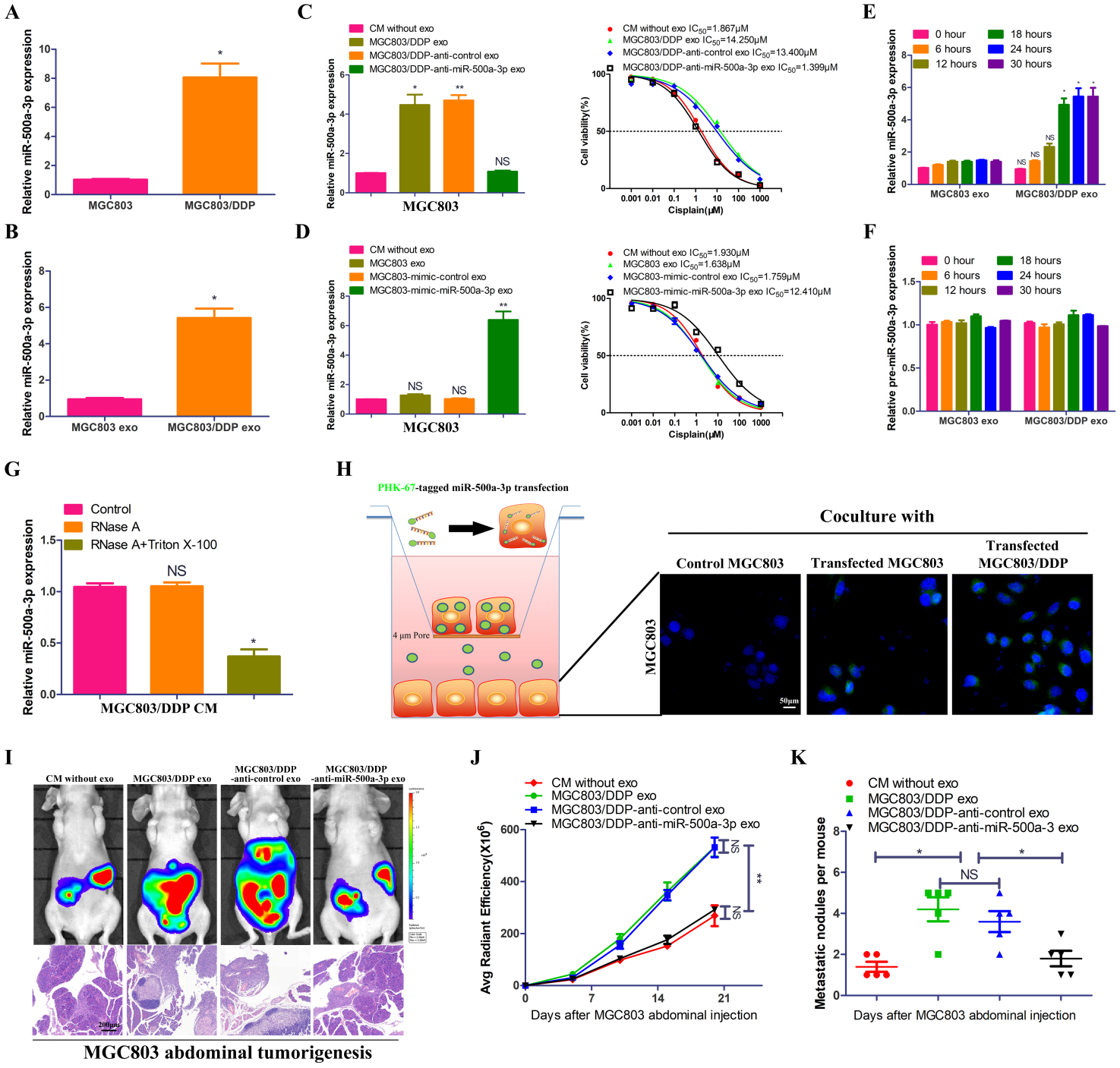

Figure 3

MGC803/DDP-derived exosomes enhances DDP resistance of MGC803 recipient cells via exosome-mediated delivery of miR-500a-3p in vitro and in vivo. A, B Real-time qRT-PCR analysis of miR-500a-3p expression in MGC803, MGC803/DDP and their corresponding exosomes. C, D Real-time qRT-PCR analysis of miR-500a-3p expression in MGC803 cells treated by indicated conditions and their corresponding proliferation assay analysis as well as IC50 value under DDP treatment. E, F Real-time qRT-PCR analysis of miR-500a-3p or pre-miR-500a-3p expression in MGC803 cells treated by MGC803

exosomes or MGC803/DDP exosomes at indicated time. G Real-time qRT-PCR analysis of miR-500a-3p expression in the culture medium(CM) of MGC803/DDP after treatment with RNase (2 μg/ml) alone or combined with Triton X-100 (0.1%) for 20 min. H MGC803 or MGC803/DDP cells transfected with the PHK-67-miR-500a-3p mimic (green fluorescence) were placed in the upper chamber and coincubated with MGC803 cells seeded in the lower chamber in a transwell system with a 0.4 μm pore membrane. After coincubation for 30 hours, MGC803 cells in the lower chamber were examined by the fluorescence microscope. I Representative bioluminescent images and microscopy observations showed effects of CM without exosomes or indicated MGC803 cell-derived exosomes on abdominal tumorigenesis under DDP treatment. J, K Comparison of bioluminescent signals and abdominal metastatic nodules after indicated treatment, five nude mice in each group. *p < 0.05, **p < 0.01.

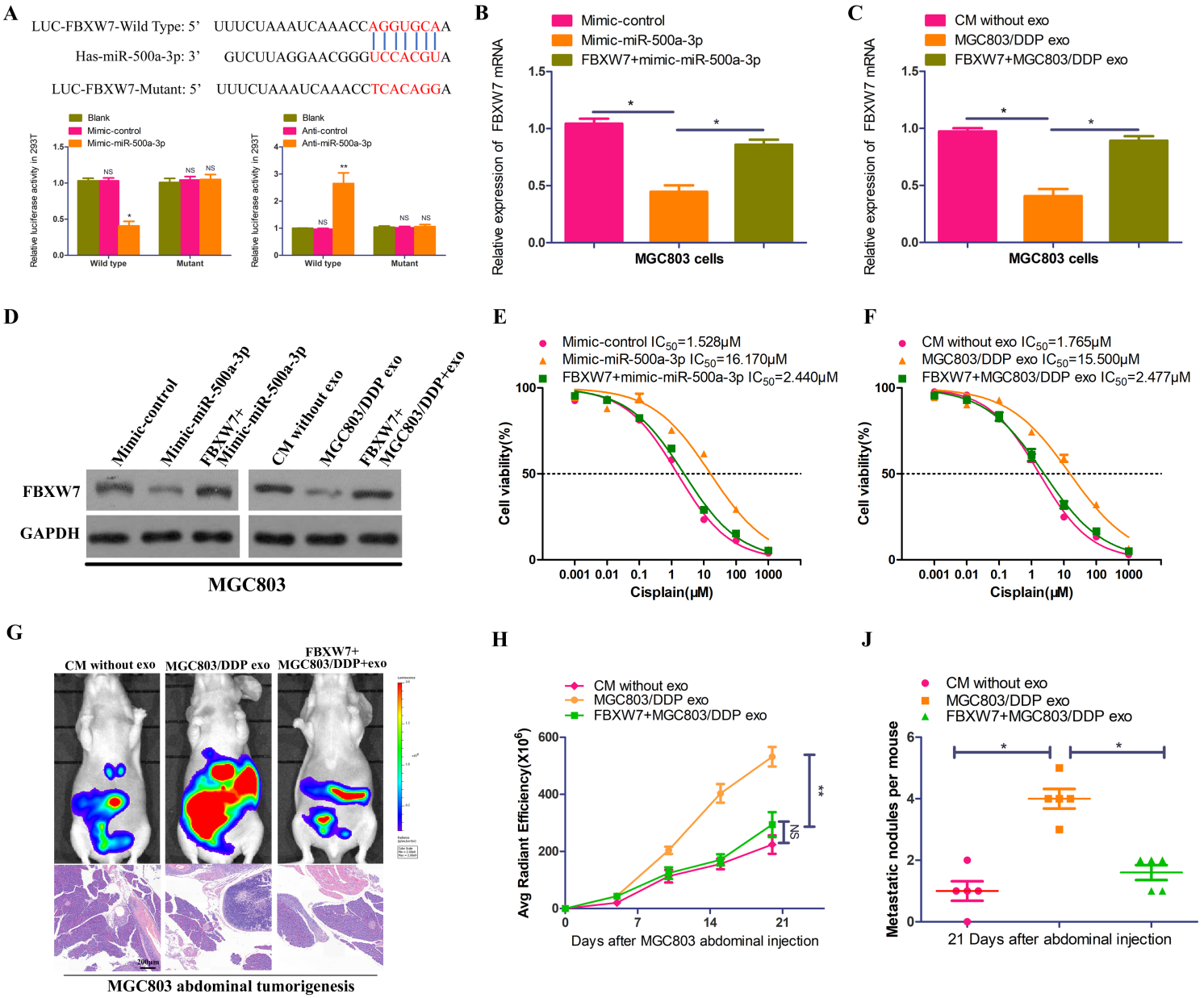

Figure 4

MGC803/DDP-derived exosomal miR-500a-3p confers DDP resistance in recipient MGC803 cells via inhibiting FBXW7. A Sequences of miR-500a-3p and the potential miR-500a-3p-binding sites at the 3'UTR of FBXW7, including nucleotides mutated in FBXW7–3'-UTR. Seed sequences are marked. Also shown effects of Blank, mimic or anti-miR-500a-3p and corresponding control on the luciferase activity of FBXW7 3'UTR-Wild Type and FBXW7 3'UTR-Mutant by dual-luciferase reported assay in 293T cells. B-D Expression of FBXW7 in MGC803 or FBXW7 overexpressed MGC803 cells transfected with mimic-control or mimic-miR-500a-3p by Real-time qRT-PCR(B) and western blot analysis(D). Expression of FBXW7 in MGC803 or FBXW7 overexpressed MGC803 cells cocoltured with CM without exosomes or MGC803/DDP exosomes by Real-time qRT-PCR(C) and western blot analysis(D). E Proliferation assay analysis and IC50 value in MGC803 or FBXW7 overexpressed MGC803 cells transfected with mimic-control or mimic-miR-500a-3p. F Proliferation assay analysis and IC50 value in MGC803 or FBXW7 overexpressed MGC803 cells cocoltured with CM without exosomes or MGC803/DDP exosomes. G Representative bioluminescent images and microscopy observations showed effects of CM without exosomes, MGC803/DDP exosomes on abdominal tumorigenesis by MGC803 or FBXW7 overexpressed MGC803 cells abdominal tumorigenesis under DDP treatment. H, J Comparison of bioluminescent signals and abdominal metastatic nodules after indicated treatment, five nude mice in each group. *p < 0.05, **p < 0.01.

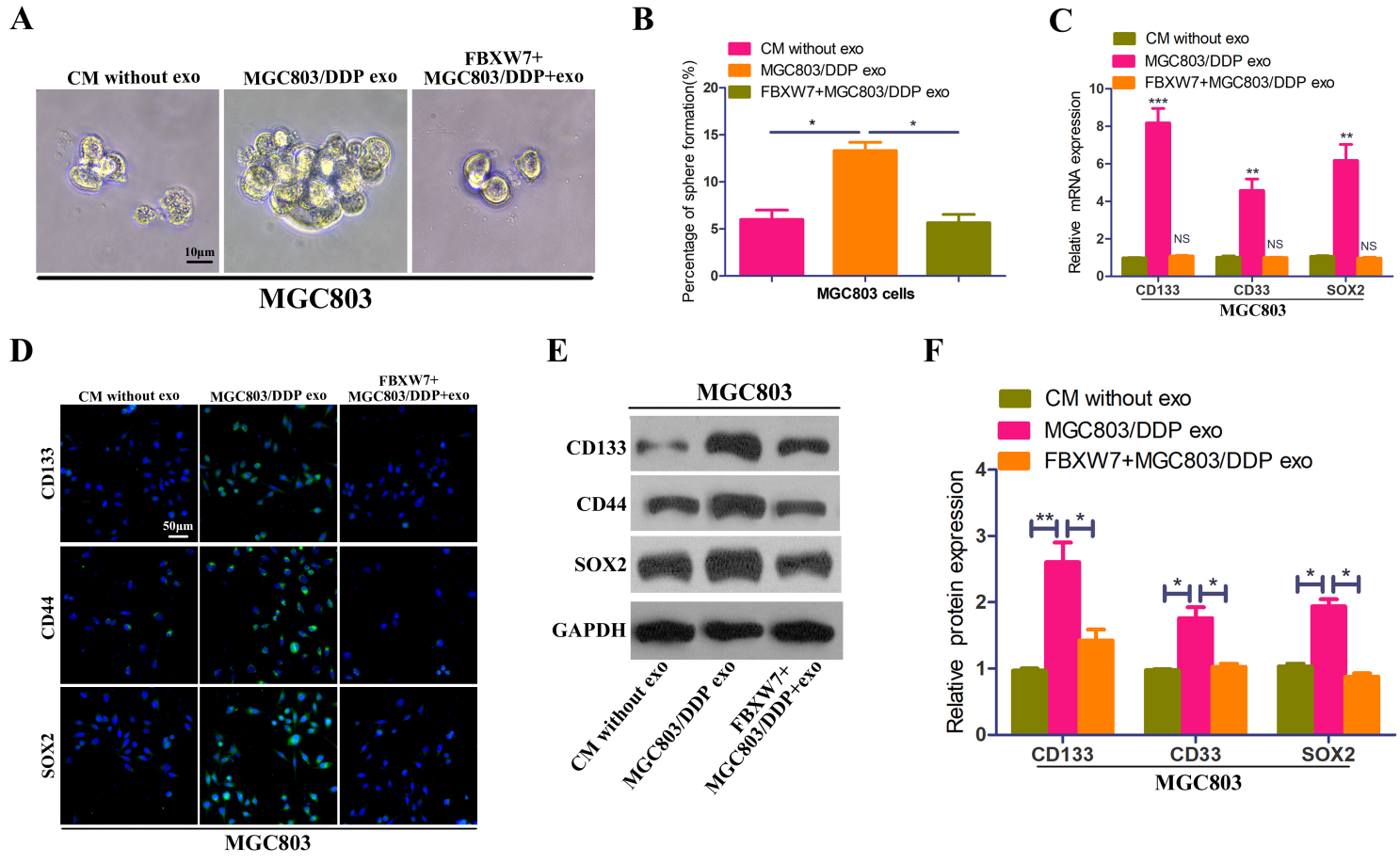

Figure 5

FBXW7 reverse the DDP resistance of exosomal miR-500a-3p by inhibiting CSCs properties. A, B Effect of CM without exosomes, MGC803/DDP exosomes on sphere formation in MGC803 or FBXW7 overexpressed MGC803 cells. C Relative mRNA expression of stemness markers CD133, CD44 and SOX2 in MGC803 or FBXW7 overexpressed MGC803 cells cocultured with CM without exosomes or MGC803/DDP exosomes. D-F Expression level of stemness markers in indicated GC cells by confocal microscopy(D) and western blot(E, F). *p < 0.05, **p < 0.01, ***p < 0.001

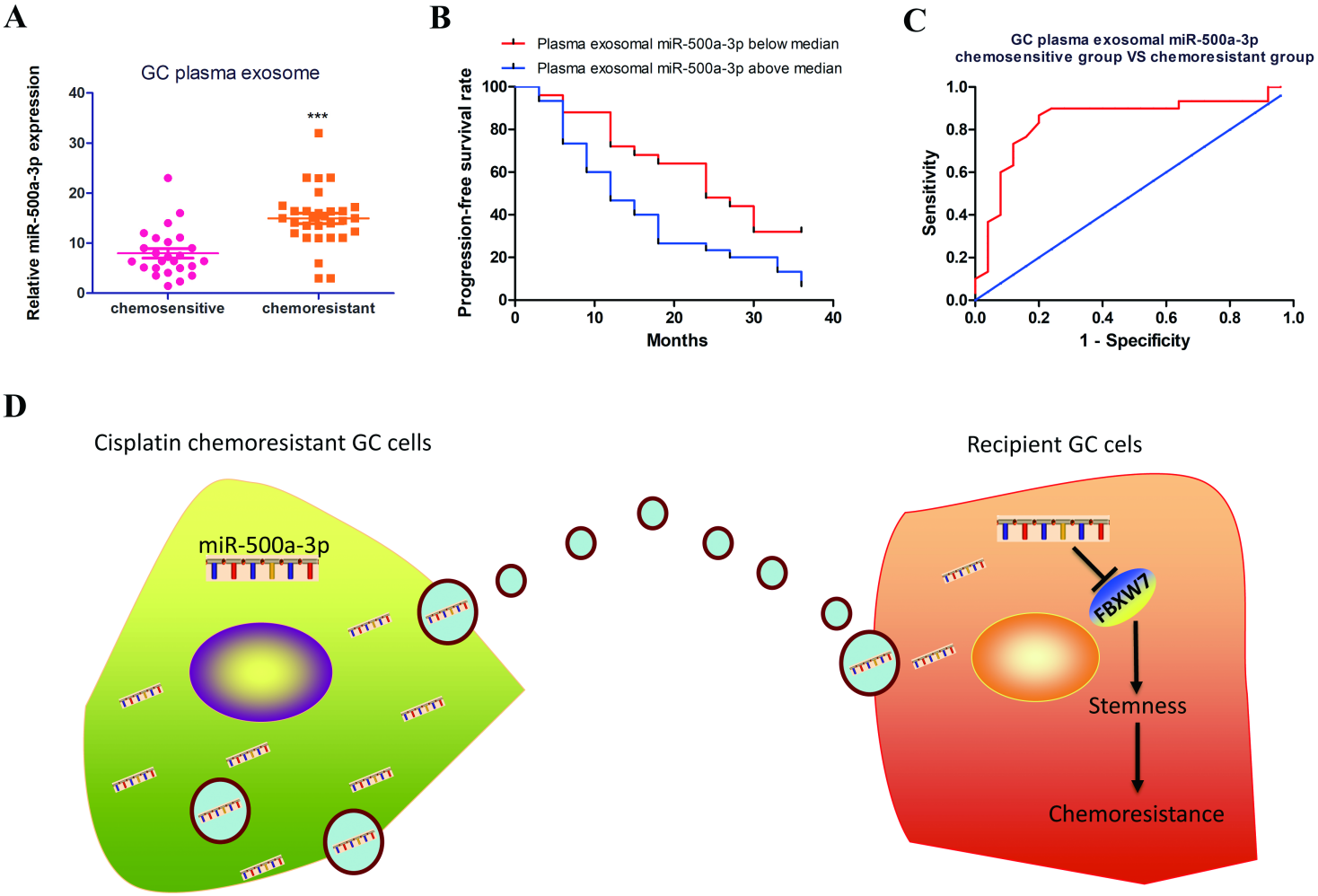

Figure 6

Plasma exosomal miR-500a-3p is related to DDP resistance in III stage GC patients. A Plasma exosomal miR-500a-3p level was detected in III stage GC patients responding or not responding to DDP treatment by real time qRT-PCR. B Kaplan-Meier analysis of 3 years progression-free survival rate in III stage GC patients from high(n=30) and low(n=25) miR-500a-3p groups, according to the median exosomal miR-500a-3p level in pre-gastrectomy plasma. C ROC curve analysis of plasma exosomal miR-500a-3p expression for discriminating the DDP resistant group (n = 30) from the sensitive group (n = 25). AUC, area under the curve. D Schematic diagram of the potential roles of exosomal miR-500a-3p in GC DDP resistance. Briefly, the DDP-resistant GC cell-secreted exosomes containing miR-500a-3p can be taken up by surrounding DDP sensitive GC cells and subsequently downregulate FBXW7 to enhance DDP resistance as well as CSCs properties of the recipient GC cells. ***p < 0.001

Supplementary Files

This is a list of supplementary files associated with this preprint. Click to download.

- TableS1.docx